3. W. M. Sinton, A. T. Tokunaga, E. E. Becklin, I. Gatley, T. J. Lee, C. J. Lonsdale, *Science* **210**, 1015 (1980); D. Morrison and C. M. Telesco, *Icarus* **44**, 226 (1980).
4. D. L. Matson, G. A. Ransford, T. V. Johnson, *J. Geophys. Res.* **86**, 1664 (1981). Using both eclipse and spectral data, Matson *et al.* made the first estimate of total heat flow from Io's hotspots and showed that anomalous emission has been occurring for at least a decade.
5. F. C. Witteborn *et al.*, *Science* **203**, 643 (1979); W. M. Sinton *Astrophys. J.* **235**, L49 (1980).
6. W. M. Sinton *et al.*, *Icarus* **54**, 133 (1983).
7. W. M. Sinton, *J. Geophys. Res.* **86**, 3122 (1981).
8. C. F. Yoder and S. J. Peale, *Icarus* **47**, 1 (1981); P. J. Cassen *et al.*, in *Satellites of Jupiter*, D. Morrison, Ed. (Univ. of Arizona Press, Tucson, 1982), pp. 93–128.
9. The principle of using spectral information to separate the hotspot and background components was used by Matson *et al.* (*4*) and Sinton (*7*) in their estimates of heat flow, but no longitude coverage was available for their analyses.
10. Data were taken using a 6- or 8-arcsec aperture in the standard chopping mode of infrared photometry. The aperture size was chosen so that a 6-arcsec aperture was used when seeing was 2-arcsec or less and the 8-arcsec aperture was used during the infrequent times when seeing was 2 to 3 arcsec. The chopper throw was 8 arcsec when the 6-arcsec aperture was being used and 10 arcsec when the 8-arcsec aperture was used. At all times the chopping direction was oriented perpendicular to the line that joined the satellite and Jupiter.
11. The primary standard for the infrared photometry was Alpha Boötes. The relative magnitude of Alpha Boötes and the flux density corresponding to zero magnitude derives from the Alpha-Lyrae–based magnitude system in A. Tokunaga, *Astron. J.* **89**, 172 (1984): 1.16×10^{-16} W cm^{-2} μm^{-1} at 10.0 μm and 7.4×10^{-18} W cm^{-2} μm^{-1} at 20.0 μm. An extrapolation using a 9400 K blackbody flux distribution (consistent with Tokunaga's calibration) was used to obtain the flux densities of zero magnitude at 8.7 μm.
12. Data taken in the broad band-passes were corrected to monochromatic flux densities using the known filter characteristics and estimates of the effects of telluric water on the atmospheric transmission. Estimates of the amount of precipitable water vapor in one air mass were made using average values at Mauna Kea of 1 mm/air mass on relatively dry nights and 5 mm/air mass on wet nights. The judgment of a wet or dry night was made on the basis of relative humidity readings at the observatory, the 10 μm/20 μm flux ratio for the standard star, and the extinction coefficient derived from 20-μm observations of the standard star.
13. D. Morrison and N. D. Morrison, in *Planetary Satellites*, J. A. Burns, Ed. (Univ. of Arizona Press, Tucson, 1977), pp. 363–378; radius assumed was 1815 km [M. E. Davies and F. Y. Katayama, *J. Geophys. Res.* **86**, 8635 (1981)]; average geometric albedo = 0.6; phase integral $q = 0.9$ [D. Morrison, in *Planetary Satellites*, J. A. Burns, Ed. (University of Arizona Press, Tucson, 1977), p. 269]. Two major uncertainties in modeling the background flux are the value of the Bond albedo (D. Simonelli and J. Veverka, *Icarus*, in press) and the variation of brightness temperature with wavelength [D. L. Matson *et al.*, *Bull. Am. Astron. Soc.* **15**, 852 (1983)]. The amount of low albedo material on the surface will also affect the background spectrum since these areas will be warmer than the model for the average disk used here. However, the exact percentage of such dark surface is not known nor the fraction of such areas which are heated chiefly by volcanic activity rather than insolation. Variations in these properties may change the estimates of the extra hotspot flux needed to fit the short wavelength data but will not affect the conclusions about the general pattern of hotspot distribution.
14. R. H. Brown *et al.*, *Icarus* **52**, 188 (1982).
15. This is in agreement with the 20-μm data of D. Morrison, in *Planetary Satellites*, J. A. Burns, Ed. (Univ. of Arizona Press, Tucson, 1977), pp. 269–301.
16. For each longitude the model calculates the total emission spectrum from Io, using the projected areas of each hotspot and summing the flux from that spot with that from the ambient background and the other hotspots [see also (*7*)].
17. J. Pearl, personal communication.
18. The same flux levels could also be modeled by increasing the area of volcanic material exposed in the Loki region. For instance, a region just north of Loki, Amaterasu Patera, was not measured by the IRIS but has albedo and color characteristics similar to other Voyager hotspots (A. McEwen, personal communication). If this region has a temperature of 400 to 450 K, the same results shown in curves c of Fig. 2 can be obtained for these three wavelengths with no change in Loki itself. This is not an exact equivalence. Further observations and analyses of data at other wavelengths may be able to constrain these models more tightly.
19. The general distribution of hotspots suggested here is consistent with the 5-μm variation with longitude reported by Sinton *et al.* (*6*), although the 5-μm pattern is confused by the variations in reflected sunlight (Fig. 1) and the time variability of the small hot sources. Also, as expected from our data, thermal emission from Io is higher at eclipse disappearances than at reappearances [D. Morrison and D. P. Cruikshank, *Icarus* **18**, 224 (1973)], suggesting more hotspot activity in the trailing hemisphere generally [W. M. Sinton *et al.*, *Bull. Am. Astron. Soc.* **15**, 851 (1983)].
20. A. S. McEwen and L. A. Soderblom, *Icarus* **55**, 191 (1983).
21. The actual near infrared spectrum is complicated both by the time variable contributions from small hot sources (*6*) and by absorbtion features in the reflected sunlight [see G. T. Sill and R. N. Clark, in *Satellites of Jupiter*, D. Morrison, Ed., (Univ. of Arizona Press, Tucson, 1982), pp. 174–212].
22. The orbital phase coverage for Io is summarized as follows: 50 to 64 deg. 19 July, 74 to 111 deg. 21 July, 235 to 271 deg. 20 July, 316 to 328 deg. 18 February, 326 to 340 deg. 7 August 1983 [UT]. Additional phase coverage was obtained from the following sources: 35 deg. 12 April 1980, D. Morrison and C. M. Telesco in (*3*); 36 deg. 24 April 1981, W. M. Sinton in (*3*); and 339 deg. 6 March 1983, W. M. Sinton in (*6*).
23. We thank John Pearl for a critical review and several helpful suggestions for improvements. We also thank Alan Tokunaga, who worked with us to prepare the plans for this program and helped acquire some of the data, C. Kaminski for his help with the telescope and equipment, and W. Sinton for allowing us to use some of his recent data in advance of publication. Martha Hanner shared valuable telescope time from another program, allowing us to acquire some of our coverage. A portion of this work was carried out at the Jet Propulsion Laboratory, California Institute of Technology under contract to NASA.

RESEARCH ARTICLE

The Precursor of the Cretaceous-Tertiary Boundary Clays at Stevns Klint, Denmark, and DSDP Hole 465A

M. Kastner, F. Asaro, H. V. Michel
W. Alvarez, L. W. Alvarez

The mass extinction of organisms at the end of the Cretaceous, about 65 million years ago, has given rise to numerous hypotheses. In 1979 a new catastrophic hypothesis to explain this extinction was proposed by Alvarez *et al.* (*1*). They suggested that an Apollo asteroid about 10 km in diameter collided with Earth and that the dust ejected from the impact reached the stratosphere and caused both temperature changes and darkness lasting several months; this event would have suppressed photosynthesis and led to the collapse of most food chains (*1, 2*). The first chemical evidence for such an impact was the discovery of anomalously high concentrations of iridium and other platinid and siderophile elements in Cretaceous-Tertiary (K/T) marine boundary clay-rich layers, both at Stevns Klint, Denmark, and in the Umbrian Apennines, near Gubbio, Italy (*3, 4*). These elements are generally depleted in Earth's crust relative to their cosmic abundances. The observed iridium concentrations at the above localities were 160 and 30 times, respectively, the average terrestrial concentration. Since then, similar geochemical anomalies have been determined by researchers at several laboratories in marine and nonmarine sediments at K/T boundary layers, recovered from more than 50 sites around the world. (*5–10*). These results were recently summarized by Alvarez *et al.* (*2*).

At present, the impact of a large extraterrestrial object, a chondritic meteorite, is widely accepted as the most plausible explanation for the worldwide iridium anomaly at the end of the Cretaceous (*2, 5, 8, 10–14*). It remains to be established whether the biological extinction and the

M. Kastner is at Scripps Institution of Oceanography, La Jolla, California 92093. F. Asaro, H. V. Michel, and L. W. Alvarez are at the Lawrence Berkeley Laboratory, University of California, Berkeley 94720. W. Alvarez is at the Department of Geology and Geophysics, University of California, Berkeley.

Table 1. Description of two marine Cretaceous-Tertiary boundary sites, their iridium anomalies, and the Pt/Ir and Au/Ir ratios at Stevns Klint and in type I carbonaceous chondrites.

Site	Location	Peak iridium abundance (ppb)	Maximum integrated amount of iridium (10^{-9} g/cm^2)	Pt/Ir	Au/Ir
Stevns Klint, Denmark	55°16.7′N, 12°26.5′E	87	336	2.01 ± 0.07	0.281 ± 0.007
DSDP Leg 62, Hole 465A, North Pacific	33°49.23′N, 178°55.14′E	15	319		
Type I carbonaceous chondrite*				1.99 ± 0.08	0.296 ± 0.018

*Reference values for C1 chondrites were obtained as follows. The value for Au/Ir is the mean of eight measurements by Krähenbuhl *et al.* (*60*). The error is the standard deviation in the mean. The value for Pt/Ir is the mean of four numbers (1.89, 1.96, 2.04, and 2.06), determined, respectively, by combining (i) M. Ebihara's (*61, 62*) platinum abundance of 0.97 ± 0.11 ppm with Krähenbuhl *et al.*'s iridium value, (ii) Ehmann and Gillum's (*63*) mean value for platinum and Krähenbuhl *et al.*'s iridium value, (iii) Ehmann and Gillum's value for both platinum and iridium, and (iv) Mason's (*64*) platinum value with Krähenbuhl *et al.*'s gold value. The overall error was taken as the standard deviation of the mean in three independent measurements, with an assumed 10 percent uncertainty in each.

asteroid impact were synchronous, and, if so, whether they were coincidental or were linked by a cause-and-effect relation.

As yet, it is not known which minerals contain the bulk of the excess siderophile metals found in the K/T boundary clay layers. Alvarez *et al.* (*2–4*) argued against the hypothesis that the high concentrations reflect a normal rate of iridium deposition during periods in which drastically reduced carbonate sedimentation rates gave rise to the clay-rich layers (*15, 16*). These arguments received further support from the report of an iridium anomaly in nonmarine sediments at the palynological K/T boundary of northeastern New Mexico and southeastern Colorado (*10*).

Commonly occurring noncalcareous phases in K/T boundary layers, in addition to clay minerals, are quartz, feldspars, and pyrite. The origin of these phases and of several additional minor ones, such as iron aluminosilicate and sanidine spherules (*17–20*), CuS and zeolites (*19*), has not been established. To gain more insight into the nature of the suggested chondritic meteorite impact, it seems essential to identify and distinguish between detrital, biogenic, authigenic, cosmogenic, and impact phases in the boundary layers. In this article results bearing on the origin of the clay minerals from two K/T boundary layers are presented. They support the meteorite impact theory.

Abstract. *Results of detailed mineralogical, chemical, and oxygen isotope analyses of the clay minerals and zeolites from two Cretaceous-Tertiary (K/T) boundary regions, Stevns Klint, Denmark, and Deep Sea Drilling Project (DSDP) Hole 465A in the north central Pacific Ocean, are presented. In the central part of the Stevns Klint K/T boundary layer, the only clay mineral detected by x-ray diffraction is a pure smectite with >95 percent expandable layers. No detrital clay minerals or quartz were observed in the clay size fraction in these beds, whereas the clay minerals above and below the boundary layer are illite and mixed-layer smectite-illite of detrital origin as well as quartz. The mineralogical purity of the clay fraction, the presence of smectite only at the boundary, and the $\delta^{18}O$ value of the smectite (27.2 ± 0.2 per mil) suggest that it formed in situ by alteration of glass. Formation from impact rather than from volcanic glass is supported by its major element chemistry. The high content of iridium and other siderophile elements is not due to the cessation of calcium carbonate deposition and resulting slow sedimentation rates. At DSDP Hole 465A, the principal clay mineral in the boundary zone (80 to 143 centimeters) is a mixed-layer smectite-illite with ≥90 percent expandable layers, accompanied by some detrital quartz and small amounts of a euhedral authigenic zeolite (clinoptilolite). The mixed-layer smectite-illite from the interval 118 to 120 centimeters in the zone of high iridium abundance has a very low rare earth element content; the negative cerium anomaly indicates formation in the marine environment. This conclusion is corroborated by the $\delta^{18}O$ value of this clay mineral (27.1 ± 0.2 per mil). Thus, this mixed-layer smectite-illite formed possibly from the same glass as the K/T boundary smectite at Stevns Klint, Denmark.*

Localities Studied

The two K/T boundary sites studied here (Table 1) are now, and were 65 million years ago, geographically widely separated from each other. At both localities the sediments are marine; the Danish section is now exposed on land, but that encountered in Hole 465A in the north Pacific Ocean has never been exposed to a meteoric water environment.

The Stevns Klint, Denmark, section is the type locality of the Danian. A thin marl layer, precisely at the K/T boundary, is known as the Fish clay. Christensen *et al.* (*21*) reported that the main clay mineral is a mixed-layer smectite-illite (S/I) with a high percentage of expandable layers and is probably of diagenetic origin. On the basis of internal bedding, Christensen *et al.* subdivided the Fish clay into four beds from bottom, bed II, to top, bed V. Bed II is underlain by Maastrichtian chalk (bed I), and bed V is overlain by a carbonate sequence called the Cerithium limestone (bed VI). Beds III and IV have the lowest $CaCO_3$ content. On the basis of the high concentration of smectite in the Fish clay, Valeton (*22*) suggested a derivation from volcanic ash. All beds of the Fish clay contain anomalously high concentrations of iridium and other siderophile elements (*1, 7*), with the largest anomalies in beds III and IV (Fig. 1).

Deep Sea Drilling Project (DSDP) Hole 465A was drilled on Hess Rise in the central north Pacific at a water depth of 2161 m. Unfortunately, rotary drilling disturbed the core. The K/T boundary was identified in core 3, section 3, at about 62.3-m subbottom depth. The iridium enrichment is smeared over an interval greater than 40 cm and is associated with both pyrite-rich dark blobs and the light-colored clayey-calcareous fraction (*7, 9*) (Fig. 2). The smearing due to the drilling placed Tertiary and Cretaceous sediments side by side, and it is not possible to say to the nearest centimeter where the base of the clayey-calcareous fraction or the base of the pyrite-rich blobs or lenses was prior to coring. The base appears to be in the vicinity of 144

cm. The original maximum integrated amount of iridium in DSDP Hole 465A, if we take into account the smearing, is very nearly the same as in the Stevns Klint section (Table 1). In fact, for these measured elements, which are enhanced by at least a factor of 5 in the clayey-calcareous fraction relative to background, the integrated amounts of all such elements (13 in total) from Stevns Klint and DSDP Hole 465A agree as well with each other as do two independent collections from Stevns Klint (*23*).

The Pt/Ir and Au/Ir ratios from the Stevns Klint K/T boundary site agree exactly (within experimental accuracy) with the values for type I carbonaceous chondrites (Table 1). However, there is a shift in stratigraphic position between the gold and iridium peaks of ~2 cm (Fig. 1), and this slight shifting of relative peak position is observed for many elements (*23*). Therefore, the excellent agreement with chondritic values (Table 1) is obtained because the entire central part of the Stevns Klint boundary was sampled. If only part of the boundary is considered, however, the stratigraphic shift would cause the siderophile element ratios to vary and to differ from chondritic values, which was a concern of Officer and Drake (*24*). Stevns Klint is also a particularly good section at which to study siderophile element ratios, because the elements occur in rather insoluble sulfides and the anoxic deposition would tend to preserve their abundances.

Methods

Bulk sediments and the insoluble residue fractions were analyzed by routine petrographic microscope and scanning electron microscope (SEM) with energy-dispersive x-ray attachment. Calcite was removed from sediments from below, within, and above the K/T boundary layers at Stevns Klint and in DSDP Hole 465A by treatment with sodium acetate–acetic acid buffer (*p*H 4.7). The clay size fractions (<2 μm) were separated from the insoluble residues by conventional settling methods and analyzed by x-ray diffraction, with $Cu_{K\alpha}$ radiation, before and after treatment with ethylene glycol. The percentage of expandable layers of mixed-layer S/I clay minerals was determined according to the method of Reynolds (*25*). The smectite from the K/T boundary layer at Stevns Klint was analyzed for major elements according to the method of Shapiro and Brannock (*26*). Oxygen isotope analyses of the clay minerals were carried out by the BrF_5 method (*27*). The isotopic results are reported in the conventional fashion as $\delta^{18}O$ (per mil) relative to standard mean ocean water (SMOW) (*28*). The experimental precision was ±0.2 per mil. We calculated the temperatures of formation, using the smectite-water oxygen isotope fractionation factor of Yeh and Savin (*29*). Alietti's (*30*) heating procedure was followed for the distinction of clinoptilolite from heulandite. The concentrations of siderophile and rare earth elements (REE) were determined by neutron activation analysis.

Results at Stevns Klint

X-ray diffraction analyses of (i) the clay fraction (<2 μm) (Fig. 3) and (ii) the insoluble residue fraction from below, within, and above the K/T boundary layer (Table 2) were carried out. The boundary clay fraction is mineralogically distinct; it is composed strictly of just smectite, with >95 percent expandable layers (*25*), and traces of gypsum, which formed, as can be seen under the SEM, by the oxidation of pyrite. The corresponding fractions from above and from

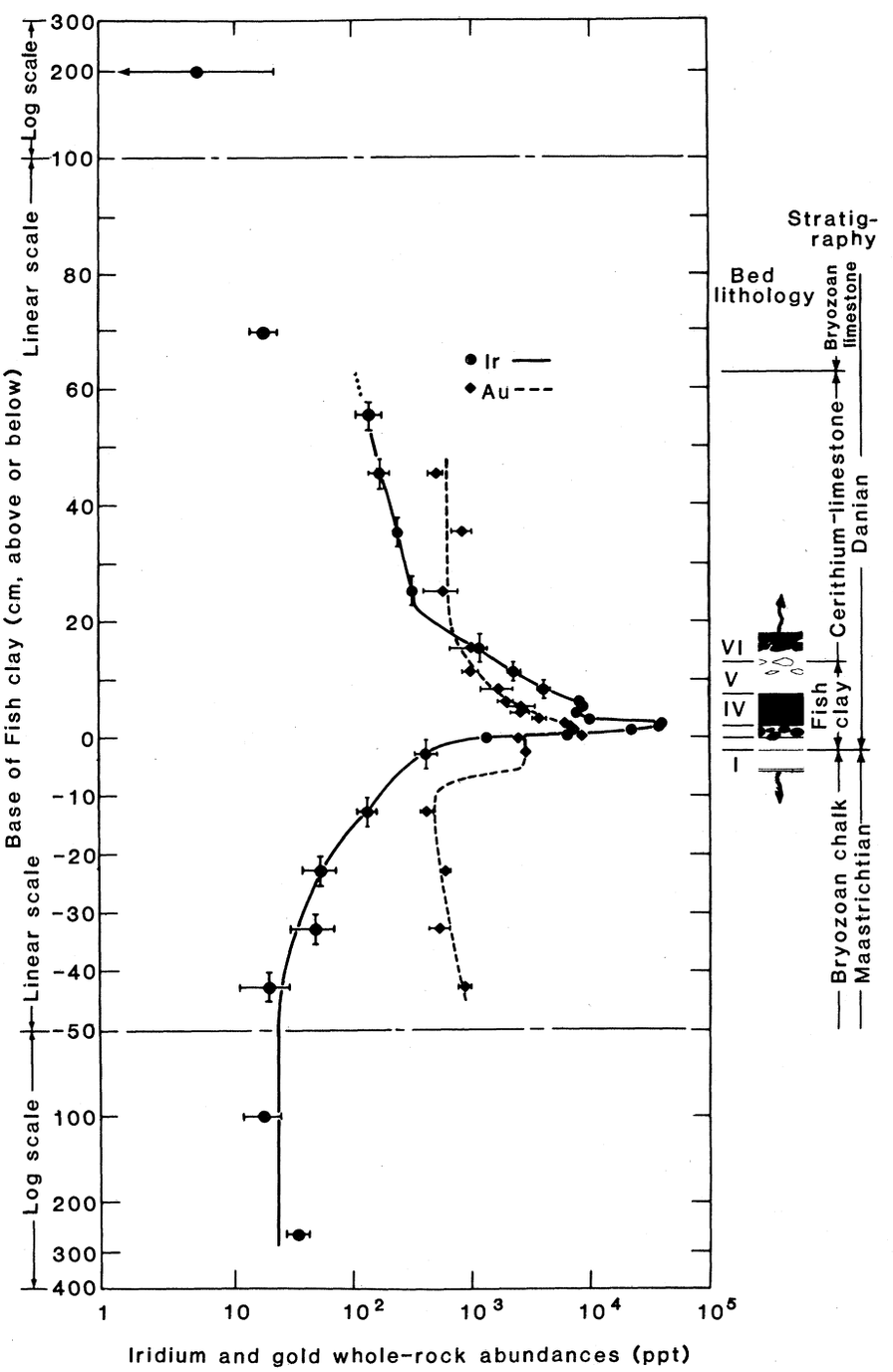

Fig. 1. Iridium and gold profiles in Cretaceous-Tertiary Stevns Klint sediments (*23*). Bed numbers are according to Christensen *et al.* (*21*).

below the boundary layer are, in contrast, composed of three main phases: a mixed-layer S/I with ~80 percent expandable layers, illite, and quartz (Fig. 3). A more detailed mineralogical study of the bulk insoluble residue fractions within the boundary Fish clay shows that bed III (*21*) and the base of bed IV are composed of almost pure smectite, whereas bed II, the top of bed IV, and bed V contain a higher amount of quartz, feldspar, and illite (Table 2). As the highest iridium and gold abundances were also found in bed III and the base of bed IV, the relation with the nearly pure smectite seems more than coincidental.

Other noncarbonate minerals present in the Fish clay are pyrite with some gypsum, carbonate-apatite in beds V and VI, and traces of barite. Varekamp and Thomas (*19*) also found rare aluminum- and iron-rich aluminosilicate spheres.

The pure smectite layers of beds III and IV, which do not contain detectable amounts of the generally ubiquitous detrital illite, indicate formation by alteration of some type of silicate, most likely glass. The presence of only traces of quartz in the bulk insoluble residue fraction points to rather rapid deposition. Thus, the high siderophile element content of these layers is not due to slow sedimentation rates after cessation of $CaCO_3$ deposition. There is, of course, no way to exclude the possibility of redeposition. However, under this assumption it is difficult to explain the unusual composition of this boundary layer smectite.

Alteration of volcanic ash has been proposed as the mode of origin of the pure smectite composing the clay fraction of the K/T boundary layer at Nye Kløv, near Stevns Klint, Denmark (*31*).

To determine the diagenetic history of the smectite from K/T boundary layer and permit a comparison with mixed-layer S/I occurring 2 m above the boundary, we carried out oxygen isotope analyses of both clays (Table 3). The smectite $\delta^{18}O$ value of 27.2 per mil (SMOW) (*28*) indicates authigenic formation in the marine environment at about 15°C (*29*). The significantly lower $\delta^{18}O$ value of the mixed-layer S/I above the boundary layer indicates formation at similar low temperatures but in a meteoric water environment (continental) or formation in the marine environment at moderately more elevated temperatures, above 35° to 40°C, or formation in the marine environment at low temperatures and isotopic exchange with meteoric water during diagenesis. As the primary mode of origin of mixed-layer S/I clays is formation during burial diagenesis from smectite (*32–34*), and in a marine sediment section temperatures do not increase upward, the diagenesis of the mixed-layer S/I must therefore have taken place somewhere else. This S/I clay is thus detrital.

Despite its formation in situ in a marine diagenetic environment, the boundary layer smectite does not exhibit a negative cerium anomaly (Fig. 4) typical of seawater (*35, 36*).

The relative contribution of ions from the solution and from the parent solids depends (i) on the relative concentrations of the ions in these phases and (ii) on the water/rock ratio (W/R). In a high W/R marine diagenetic environment, commonly referred to as an open system, authigenic solid phases will acquire the seawater's chemical signatures of the oxygen isotopes as well as of the REE abundance pattern. In a low W/R regime (a closed system), however, the authigenic solid phases might still acquire the seawater's chemical signatures of major ions in the fluid phase, for example, oxygen. Concentrations of minor and trace elements, such as REE, which are more abundant in the solid phases, would, however, be controlled by the solid phases. Hence, the absence of a negative cerium anomaly in the smectite suggests formation in a low W/R diagenetic system.

The important conclusion that the smectite formed in a low W/R (closed) diagenetic system suggests that the

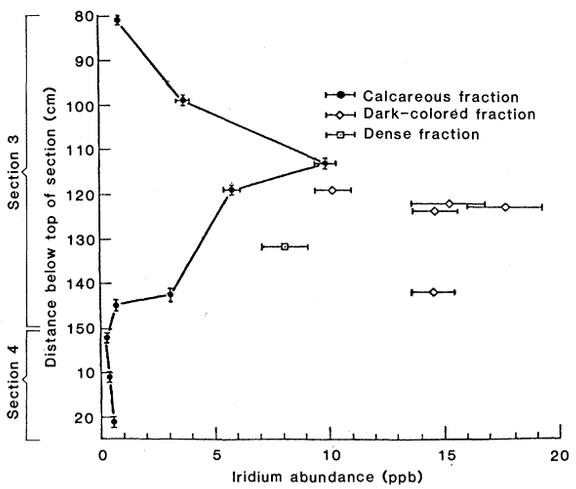

Fig. 2. Iridium profile across the Cretaceous-Tertiary boundary, DSDP Hole 465A [from Alvarez *et al.* (*2*), figure 2b].

Table 2. Mineralogy of silicates in the noncalcareous fraction at Cretaceous-Tertiary boundary region sediments, Stevns Klint, Denmark; tr, trace; x, some; xx, present; xxx, abundant.

Sample		Quartz	Feldspar	Smectite	Illite
Bed*	Distance from base of bed (cm)				
VI	10–15†	xx		xx	
VI‡	0–5	xx	x	xxx	x
V	3–6	tr		xxx	
V	0–3	xx	x	xx	
IV	4–5	x		xxx	tr
IV	3–4	x	tr	xx	tr
IV	2–3	xx		xxx	tr
IV	1–2	x		xxx	
IV	0.5–1.0	x		xxx	tr
IV	0.0–0.5	tr§		xxx	
III	0–1	tr§		xxx	
II	0.5–1.0	xx	x	xxx	x
II	0.0–0.5	xxx	tr	xx	tr
I	45–50	xx	xx	xx	x
I	35–40	xxx	xxx	x	tr

*Bed numbers are according to Christensen *et al.* (*21*). †In bed VI (10 to 15 cm), carbonate-apatite is a rather abundant phase; its abundance increases at 20 to 25 cm and 30 to 35 cm and decreases again at 40 to 45 cm. The abundance of smectite decreases and of quartz increases in this bed from sample (10 to 15 cm) to sample (40 to 45 cm). ‡A few samples in beds V and VI contain traces of mixed-layer smectite-illite, not shown in the table. §Quartz was not detected in the clay size fraction; some quartz was observed in the >2-μm size fraction.

Table 3. Oxygen isotope values of clay minerals.

Sample	Clay mineral†	$\delta^{18}O$ (per mil) (SMOW)	Comments
DPDS Hole 465A, core 3, section 3, 118 to 120 cm	Smectite-illite, ≥90% expandable layers	27.1 ± 0.2	K/T boundary
Stevns Klint, bed IV*, 0.0 to 0.5 cm	Smectite, >95% expandable layers	27.2 ± 0.2	K/T boundary
Stevns Klint, 2 m above K/T layer	Smectite-illite, ~80% expandable layers	22.7 ± 0.2	Tertiary

*Bed numbers are according to Christensen *et al.* (*21*). †The percentage of expandable layers was determined according to the method of Reynolds (*25*).

Table 4. Major-element composition of smectite and spheres from the Cretaceous-Tertiary boundary layer at Stevns Klint, Denmark, of microtektites, and of representative marine smectites (percent by weight). Total iron is expressed as FeO; N.D., not determined.

Oxide	Smectite (<2 μm), Stevns Klint	Spheres, Stevns Klint (*19*)		Microtektite				Smectite in pillow basalt, Peru Trench§	Hydrothermal smectite, Loihi submarine volcano‖	Iron smectite in volcanogenic sediments, Indian Ocean¶	Beidellite in volcanogenic sediments, Indian Ocean**	Iron saponite in volcanogenic sediments, Indian Ocean††
		27 μm	37 μm	Indian Ocean*	Indian Ocean*	East China Sea†	(Bottle green) Indian Ocean‡					
SiO_2	60.00	59.62	64.34	60.7	59.9	62.7	60.8	43.25	52.7	60.1	64.7	61.0
Al_2O_3	17.07	17.04	17.89	18.4	19.3	16.6	17.1	5.79	0.90	5.79	21.4	13.1
FeO	4.20	10.23	4.85	5.5	4.5	7.4	6.71	15.54	24.29	13.9	2.4	10.1
MgO	7.08	6.75	7.25	6.6	7.1	7.0	9.95	16.62	2.22	5.6	3.5	11.4
CaO	2.17	3.22	3.60	4.9	5.4	4.8	3.25	0.65	0.36	0.9	1.9	1.0
TiO_2	0.67	0.65	0.90	N.D.	N.D.	0.8	0.93	0.18	0.20	N.D.	N.D.	N.D.
Na_2O	N.D.	N.D.	N.D.	0.9	0.6	1.6	0.21	1.95	2.44	3.5	3.8	1.2
K_2O	N.D.	0.23	0.27	0.4	0.3	1.4	0.32	1.14	0.75	1.1	1.9	0.5

*32°06′S, 55°51′E (*51*). †28°52′N, 135°33′E (*51*). ‡08°51′S, 102°07′E (*52*). §Table 2, sample 11-1G (*43*). ‖Table 2, sample 20-1G (*50*). ¶Table 1, sample D (*48*). **Table 1, sample B (*48*). ††Table 1, sample C (*48*).

chemistry of the authigenic smectite should closely resemble the chemistry of a precursor glass (or other silicate); microtektite-like aluminosilicate spheres have been found, for example, by Varekamp and Thomas (*19*) and Montanari *et al.* (*20*). The major element composition of the smectite is presented in Table 4. A literature search of major element analyses of smectites (*37–50*) revealed that the chemical compositions of diagenetic nonmarine and diagenetic and hydrothermal marine smectites are significantly different from the chemical composition of this smectite. The boundary clay, which is a beidellitic montmorillonite, does, however, closely resemble the composition of rare aluminum- and iron-rich aluminosilicate (Table 4), most likely glassy, spherules from the boundary clay of Stevns Klint (*19*) and of several other microtektites (*51, 52*).

In summary, the pure smectite layer at the K/T boundary at Stevns Klint formed authigenically in a low W/R submarine diagenetic environment, most probably isochemically from the aluminum- and iron-rich aluminosilicate impact spherules.

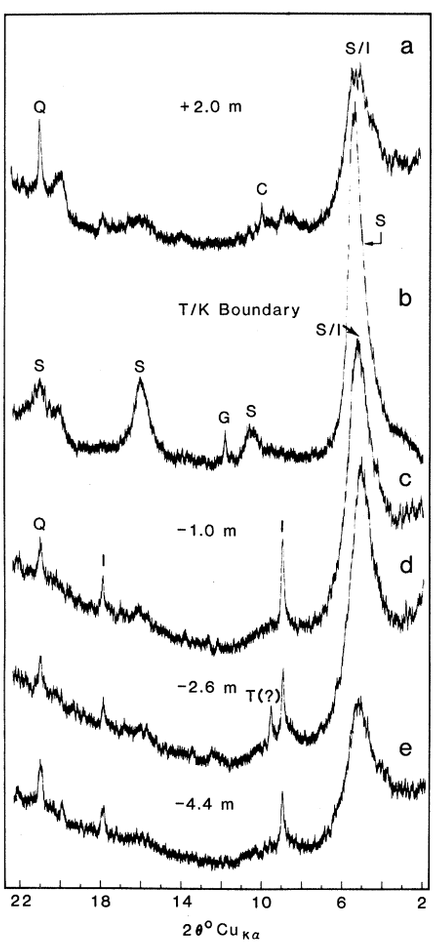

Fig. 3. X-ray diffraction patterns of the noncalcareous, clay size fraction (<2 μm) of samples treated with ethylene glycol, from below, at, and above the K/T boundary layer, Stevns Klint, Denmark. Abbreviations: S, smectite; I, illite; S/I, mixed-layer smectite-illite; Q, quartz; G, gypsum (from pyrite oxidation); C, clinoptilolite; and T, talc.

Results at DSDP Hole 465A

Unfortunately, only very small amounts of samples were available from this site for mineralogical and chemical analyses. Thus, only four samples from the smeared-out K/T boundary layer from core 3, section 3, were studied. The mineralogy of the insoluble residue is summarized in Table 5. Figure 2 shows that the highest iridium abundances in the light-colored calcareous clay layers were observed between 100 and 140 cm and in the dark pyrite-bearing clay at 118 to 125 cm and 141 to 143 cm. In these sediments, the only clay mineral is a mixed-layer S/I with ≥90 percent expandable layers; medium to small amounts of detrital quartz are also present. Small amounts of a euhedral authigenic zeolite, clinoptilolite, are present throughout the interval from 80 to 143 cm. At 143 to 144 cm, in what is probably Cretaceous sediment (deduced from the REE abundance pattern), this zeolite is a prominent component of the insoluble

residue. The most common, although by no means the only, precursor of clinoptilolite is glass (*53–55*). The transformation of smectite, which most probably formed from glass, to a mixed-layer S/I with a high percentage (≥90 percent) of expandable layers, in 65 million years, is not surprising according to the experimental results of Eberl and Hower (*56*).

This mixed-layer S/I was separated from a mixture of light and a little dark sediment from the high-iridium abundance zone at 118 to 120 cm and analyzed for its REE abundance and pattern and its $\delta^{18}O$ value. The REE abundances are very low and show the typical seawater negative cerium anomaly (Fig. 5), indicating authigenic formation in a high W/R (open) system environment. This conclusion is supported by the $\delta^{18}O$ value of the purified mixed-layer S/I [27.1 per mil (SMOW)] (Table 3). Oxygen isotope profiles of interstitial waters at DSDP sites show an average depletion gradient of 0.5 per mil per 100 m of burial (*57*). Hence, minor diagenetic alterations of marine clay minerals in the uppermost 50 m of marine sediments would barely affect their original $\delta^{18}O$ value. Interestingly, this value is identical to that of the authigenic K/T boundary smectite at Stevns Klint but clearly different from that of the detrital mixed-layer S/I from 2 m above the boundary at Stevns Klint (Table 3).

Table 5. Mineralogy of silicates in the noncalcareous fraction at Cretaceous-Tertiary boundary region sediments, DPDS Hole 465A; tr, trace, x, some; xx, present, xxx, abundant.

Sample		Interval (cm)	Quartz	Mixed-layer smectite-illite	Clinoptilolite	Comments
Core	Section					
3	3	81–82	xx	xx	x	Light tan
3	3	111–112	xx	xx	x	Light tan
3	3	118–120	tr	xx		Contains blobs enriched in pyrite
3	3	143–144	tr	x	xxx	White, with traces of dark blobs

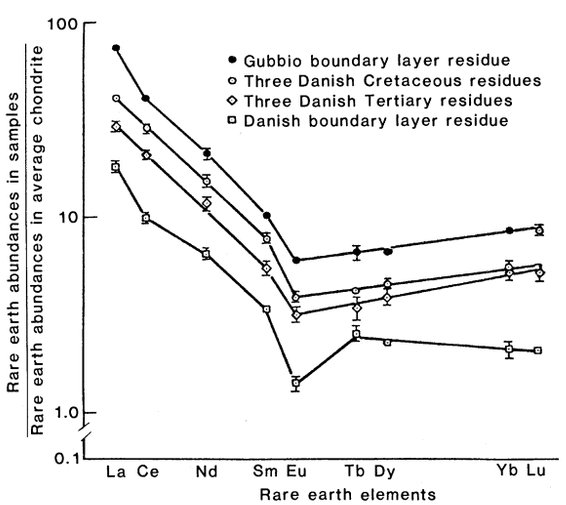

Fig. 4. The rare earth element abundance normalized to chondrites of boundary-layer residues from Danish and Italian localities (*65*). [Courtesy of the American Chemical Society, Washington, D.C.]

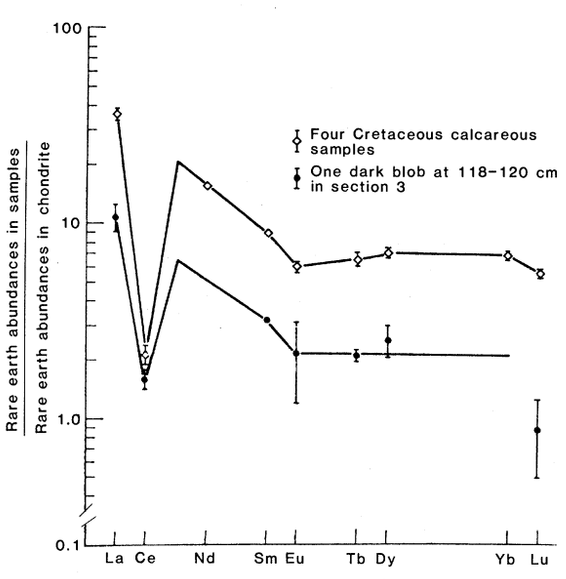

Fig. 5. Rare earth element abundance normalized to chondrite of K/T boundary sediments, DSDP Hole 465A.

We suggest that the authigenic phases at DSDP Hole 465A and Stevns Klint most probably formed from the same impact glass. They formed, however, in slightly different diagenetic regimes, the one in an open and the other in a closed marine system. As a result, these samples exhibit somewhat different mineralogy, a distinctly different REE distribution pattern, but the same $\delta^{18}O$ value of the clay minerals.

Concluding Remarks

Recently Rampino and Reynolds (*31*) suggested another nonimpact explanation for the origin of the clay minerals and the geochemical anomalies at four K/T boundary layers: Nye Kløv, Denmark; Gubbio, Italy; Caravaca, Spain; and El Kef, Tunisia. They determined the clay mineralogy of the boundary clay layers and of the carbonate sediments above and below the layers and proposed that volcanic material should be considered the cause of the geochemical anomalies.

They argued that the central criteria for an impact origin of the boundary clay layer would be the following: (i) a mixture of meteoritic and terrestrial ejecta materials (whatever that signifies) should be present; (ii) the material should be relatively homogeneous at each place and mineralogically similar at all localities; and (iii) the mineralogy of the boundary layer should contain a component that is distinct from the locally derived clays, as found in the sediments above and below it. Instead, they observed (*31*, p. 495) that "the boundary clay is neither mineralogically exotic nor distinct from locally derived clays above and below the boundary." They also showed that the clay minerals differ from place to place. The main clay mineral is either a pure smectite (Denmark) or a

mixed-layer S/I but with a difference in the percentage of expandable layers at each locality (Spain, Tunisia, Italy). It can be argued that finding "exotics," such as "meteoritic or terrestrial ejecta materials," requires more than just x-ray diffraction analysis of the <2-μm fraction. In fact, materials that definitely qualify for the description exotic, such as sanidine spherules, are plentiful in the boundary layer at Caravaca, Spain, and at several other places (*17, 20*), rare aluminum- and iron-rich aluminosilicate spheres have been observed in Stevns Klint (*22*), and potassium feldspar spheroids have been found in the boundary clay at DSDP Hole 465A (*20*).

Smectite, the most common alteration product of glass, is a metastable phase that transforms with time and temperature, through mixed-layer clay minerals, generally to illite or chlorite, or both (*32–34*). The rates of these transformations are strongly influenced by the diagenetic and tectonic histories of the sediments. The K/T boundary section of Gubbio, Italy, for example, is highly recrystallized, and the calcareous nannofossils are poorly preserved because of dissolution and recrystallization (*58*). Hence, the fact that the mixed-layer S/I contains a low percentage of expandable layers may indicate only that it is, as would be expected, in a more advanced stage of diagenesis. The admixture of detrital clay minerals in some, but not all, clay boundary layers could be due to various degrees of bioturbation. In the laminated Fish clay, in which no bioturbation occurred, the clay mineralogy of the boundary layer is indeed distinct (Fig. 3).

Rampino and Reynolds' (*31*) explanations of the observed geochemical anomalies lean on a single reference by Goldschmidt (*59*) proposing that iridium and other trace metals are enriched in some andesitic volcanic ashes, in which they occur in heavy minerals. Goldschmidt, however, did not provide any iridium data on andesitic ashes; instead, he stated (*59*, p. 691) that "very little has been published about platinum metals in rocks belonging to intermediate stages of magmatic evolution such as diorites and andesites." Although Goldschmidt's remark is 29 years old, this omission does not seem to have been remedied in the meantime.

References and Notes

1. L. W. Alvarez, W. Alvarez, F. Asaro, H. V. Michel, *Science* **208**, 1095 (1980).
2. W. Alvarez, L. W. Alvarez, F. Asaro, H. V. Michel, *Geol. Soc. Am. Spec. Pap. 190* (1982), p. 305.
3. ———, *Eos* **60**, 734 (1979).
4. ———, *Cretaceous-Tertiary Boundary Events Symposium, Copenhagen* (Univ. of Copenhagen, Copenhagen, 1979), p. 69.
5. R. Ganapathy, *Science* **209**, 921 (1980).
6. ———, S. Gartner, M. J. Jiang, *Earth Planet. Sci. Lett.* **54**, 393 (1981).
7. F. T. Kyte, Z. Zhou, J. T. Wasson, *Nature (London)* **288**, 651 (1980).
8. J. Smit and J. Hertogen, *ibid.* **285**, 198 (1980).
9. H. V. Michel, F. Asaro, W. Alvarez, L. W. Alvarez, *Init. Rep. Deep Sea Drill. Proj.* **62**, 847 (1981).
10. C. J. Orth, J. S. Gilmore, J. D. Knight, C. L. Pillmore, R. H. Tschudy, J. E. Fassett, *Science* **214**, (1981).
11. J. D. O'Keefe and T. J. Ahrens, *Nature (London)* **298**, 123 (1982).
12. ———, *Geol. Soc. Am. Spec. Pap. 190* (1982), p. 103.
13. K. J. Hsü, *Nature (London)* **285**, 201 (1980).
14. C. Emiliani, E. B. Kraus, E. M. Shoemaker, *Earth Planet. Sci. Lett.* **55**, 317 (1981).
15. D. V. Kent, *Science* **211**, 648 (1981).
16. M. R. Rampino, *Houston Lunar Planet. Inst. Snowbird Abstr. Suppl.* (1981), p. 4.
17. J. Smit and G. Klaver, *Nature (London)* **292**, 47 (1981).
18. S. Epstein, *Lunar Planet. Sci. Conf. 13th (abstr.)* (1982), p. 205.
19. J. C. Varekamp and E. Thomas, *Geol. Soc. Am. Spec. Pap. 190* (1982), p. 461.
20. A. Montanari *et al.*, *Geology* **11**, 668 (1983).
21. L. Christensen, S. Fregerslev, A. Simonsen, J. Thiede, *Bull. Geol. Soc. Den.* **22**, 193 (1973).
22. I. Valeton, *Neues Jahrb. Geol. Palaeontol. Monatsh.* **1959**, 193 (1959).
23. F. Asaro, W. Alvarez, H. V. Michel, L. W. Alvarez, M. Kastner, J. Thiede, in preparation.
24. C. B. Officer and C. L. Drake, *Science* **219**, 1383 (1983).
25. R. C. Reynolds, in *Crystal Structures of Clay Minerals and Their X-Ray Identification*, G. W. Brindley and G. Brown, Eds. (Mineralogical Society, London, 1980), p. 249.
26. L. Shapiro and W. W. Brannock, *U.S. Geol. Surv. Bull. 1144-A* (1962).
27. R. N. Clayton and T. K. Mayeda, *Geochim. Cosmochim. Acta* **27**, 43 (1963).
28. H. Craig, *Science* **133**, 1833 (1961).
29. H. W. Yeh and S. M. Savin, *Geol. Soc. Am. Bull.* **88**, 1321 (1977).
30. A. Alietti, *Am. Mineral.* **57**, 1448 (1972).
31. M. R. Rampino and R. C. Reynolds, *Science* **219**, 495 (1983).
32. E. A. Perry, Jr., and J. Hower, *Clays Clay Miner.* **18**, 165 (1970).
33. E. A. Perry, Jr., *Geol. Soc. Am. Bull.* **85**, 827 (1974).
34. J. Hower, E. V. Eslinger, M. E. Hower, E. A. Perry, *ibid.* **87**, 725 (1976).
35. E. D. Goldberg, M. Koide, R. A. Schmitt, R. H. Smith, *J. Geophys. Res.* **68**, 4209 (1963).
36. O. T. Høgdahl, S. Melson, V. T. Bowen, *Adv. Chem. Ser.* **73**, 308 (1968).
37. P. F. Kerr *et al.*, *Analytical Data on Reference Clay Materials* (American Petroleum Institute Project 49, Clay Mineral Standards, Washington, D.C., 1950).
38. G. Arrhenius, in *The Sea*, M. N. Hill, Ed. (Wiley, New York, 1963), vol. 3, p. 655.
39. J. J. Griffin, H. Windom, E. D. Goldberg, *Deep-Sea Res.* **15**, 433 (1968).
40. J. L. Bischoff, *Clays Clay Miner.* **20**, 217 (1972).
41. C. E. Weaver and L. D. Pollard, *The Chemistry of Clay Minerals* (Elsevier, New York, 1973).
42. G. R. Heath and J. Dymond, *Geol. Soc. Am. Bull.* **88**, 723 (1977).
43. K. F. Scheidegger and D. S. Stakes, *Earth Planet. Sci. Lett.* **36**, 413 (1977).
44. J. Dymond and W. Eklund, *ibid.* **40**, 243 (1978).
45. M. Hoffert, A. Perseil, R. Hekinian, P. Choukroune, H. D. Needham, J. Francheteau, X. Le Pichon, *Oceanol. Acta* **1**, 73 (1978).
46. W. E. Seyfried, Jr., W. C. Shanks III, W. E. Dibble, Jr., *Earth Planet. Sci. Lett.* **41**, 265 (1978).
47. J. R. Hein, H. W. Yeh, E. Alexander, *Clays Clay Miner.* **27**, 185 (1979).
48. A. Desprairies and C. Bonnot-Courtois, *Earth Planet. Sci. Lett.* **48**, 124 (1980).
49. M. A. Rateev, P. P. Timofeev, N. V. Rengarten, *Init. Rep. Deep Sea Drill. Proj.* **54**, 307 (1980).
50. E. H. DeCarlo, G. M. McMurtry, H. W. Yeh, *Earth Planet. Sci. Lett.* **66**, 438 (1983).
51. W. A. Cassidy, B. Glass, B. C. Heezen, *J. Geophys. Res.* **74**, 1008 (1969).
52. B. P. Glass, *ibid.* **77**, 7057 (1972).
53. R. A. Sheppard, *Adv. Chem. Ser.* **101**, 279 (1971).
54. M. Kastner and S. A. Stonecipher, in *Natural Zeolites, Occurrences, Properties, Use*, L. B. Sand and F. A. Mumpton, Eds. (Pergamon, New York, 1978), p. 199.
55. M. Kastner, in *The Sea*, C. Emiliani, Ed. (Wiley, New York, 1981), vol. 7, p. 915.
56. D. Eberl and J. Hower, *Geol. Soc. Am. Bull.* **87**, 1326 (1976).
57. J. R. Lawrence, J. Gieskes, W. S. Broecker, *Earth Planet. Sci. Lett.* **27**, 27 (1975).
58. K. Perch-Nielsen, J. McKenzie, Q. He, *Geol. Soc. Am. Spec. Pap. 190* (1982), p. 353.
59. V. M. Goldschmidt, *Geochemistry* (Clarendon, Oxford, 1954).
60. U. Krähenbuhl, J. W. Morgan, R. Ganapathy, E. Anders, *Geochim. Cosmochim. Acta* **37**, 1353 (1973).
61. W. Alvarez, F. Asaro, H. V. Michel, L. W. Alvarez, *Science* **216**, 886 (1982).
62. E. Anders, personal communication.
63. W. D. Ehmann and D. E. Gillum, *Chem. Geol.* **9**, 1 (1972).
64. J. H. Crocket, R. R. Keays, S. Hsieh, *Geochim. Cosmochim. Acta* **31**, 1615 (1967) [as given in *Handbook of Elemental Abundances in Meteorites*, B. Mason, Ed. (Gordon and Breach, New York, 1971)].
65. *Nuclear and Chemical Dating Techniques* (Symposium Series 176, American Chemical Society, Washington, D.C., 1982), p. 401.

66. We thank J. Thiede for providing samples from the K/T section, Stevns Klint, Denmark; Y. K. Bentor and two anonymous reviewers for their critical reading of the manuscript and for their constructive comments; J. D. O'Keefe for many interesting discussions about the subject; J. M. Gieskes for the chemical analysis of the smectite from Denmark; and G. Anderson for her excellent help in the laboratory. We thank T. Lim for supervising the irradiation of samples at the small Berkeley Research Reactor. This work was supported by the Director, Office of Energy Research, Office of Basic Energy Sciences, Division of Engineering, Mathematical and Geosciences, of the U.S. Department of Energy, under contract DE-AC03-765F00090; by NSF grant EAR-81-15858; and by the NASA Ames Research Center under contract A-71693B.

3 February 1984; accepted 9 May 1984